ELSEVIER

Soil Dynamics and Earthquake Engineering 24 (2004) 389–396

SOIL DYNAMICS AND EARTHQUAKE ENGINEERING

www.elsevier.com/locate/soildyn

On arrangement of source and receivers in SASW testing

Longzhu Chen[a,*], Jinying Zhu[b], Xishui Yan[c], Chunyu Song[a]

[a]*School of Civil Engng. and Mechanics, Shanghai Jiaotong University, Shanghai 200030, China*
[b]*Department of Civil and Envir. Engng., University of Illinois at Urbana-Champaign, IL 61801, USA*
[c]*College of Architecture and Civil Engng., Zhejiang Univ., Hangzhou 310027, China*

Accepted 28 December 2003

Abstract

This study investigates the effects of source and receivers arrangement on the Rayleigh wave dispersion curve in SASW testing. Analytical studies and numerical simulations with coupled finite and infinite elements are presented in this paper. It is shown that arrangement of source and receivers has a significant effect on test results, especially for soils with high Poisson's ratio or saturated soils. Larger source-to-receiver distance and receiver spacing usually give better results, and it is unnecessary to keep them equal. To satisfy the error control requirement in Rayleigh wave phase velocity measurement, source-to-receiver distance and receiver spacing should meet corresponding minimum values, which are proposed for different Poisson's ratios of soil in this paper.

Keywords: Rayleigh wave; Spectral analysis of surface wave (SASW) testing; Wave velocity; Arrangement of receivers

1. Introduction

Body waves (P and S waves) and surface waves (R wave) will be generated in soil when the surface of a uniform half-spaced elastic soil system is subjected to a vertical load excitation. Unlike P wave, the velocity of which is significantly affected by water content and saturation degree of soil, shear wave velocity V_s is mainly governed by properties of soil skeleton, and is closely related to shear modulus as well as strength of soil.

According to plane elastic wave theory, plane Rayleigh wave velocity V_R is related to shear wave velocity V_S of the material by Poisson's ratio ν. For the case of a uniform half-space, the ratio of V_R to V_S varies from 0.874 to 0.955 for values of Poisson's ratio ν ranging from 0 to 0.5. Therefore, if the V_R of a uniform layer of soil has been measured, the shear wave velocity V_S can be easily determined. For a non-uniform or layered soil system, dispersion of surface wave will occurs. Dispersion means Rayleigh wave velocity varies with frequency f, which forms the theoretical basis of the spectral analysis of surface wave (SASW) test method. The overall objective of SASW test is to measure Rayleigh wave dispersion curve and then to obtain shear wave velocity profile through inversion of dispersion curve. A schematic of the SASW test is shown in Fig. 1. The wavelength λ_R and Rayleigh wave velocity V_R can be calculated from the following equations

$$\lambda_R = \frac{2\pi\Delta x}{\Delta\varphi}, \quad V_R = \lambda_R f \tag{1}$$

where Δx and $\Delta\varphi$ are, respectively, the spacing and phase angle difference at frequency f of two receivers. In reality, ideal plane surface wave is difficult to generate. When the SASW method is used in field, a transient load is applied at a point on the surface of soil. Waves generated by the point source include Rayleigh waves that propagate along a cylindrical wave front and body waves that propagate along a hemispherical wave front. Because Rayleigh waves attenuate at a much slower rate than body waves, at a large source-to-near-receiver distance r, it can be assumed that the waves detected by the two receivers are primarily composed of Rayleigh wave components. This raises a problem in choosing proper source-to-receiver distance to make sure the required measurement and calculation precision is satisfied.

In the past two decades, lots of research has been made on the arrangement of source and receivers for the SASW method. A generally used criterion was proposed by Heisey et al. [1] on the basis of experimental studies.

* Corresponding author.
E-mail address: lzchen@sjtu.edu.cn (L. Chen).

0267-7261/$ - see front matter © 2004 Elsevier Ltd. All rights reserved.
doi:10.1016/j.soildyn.2003.12.004

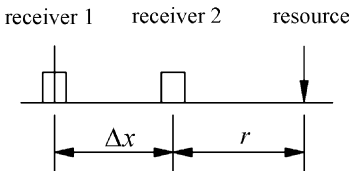

Fig. 1. Arrangement of SASW test.

They suggested for an arrangement of $r = \Delta x$, the acceptable wavelength can be expressed as $\lambda_R/3 \le \Delta x \le 2\lambda_R$. However, theoretical studies conducted by other researchers [2–5] proposed criteria that are different from the results of Heisey et al. [1] Sanchez-Salinero et al. [2] suggested $r = \Delta x$, and $\Delta x > 2\lambda_R$. With transfer matrix method, Rosset et al. [3] investigated the dispersion of Rayleigh waves caused by point load, and proposed the following criteria: $0.5r \le \Delta x \le r$, and $0.5\lambda_R \le r \le 2\lambda_R$. Gucunski and Woods [5] used finite element method to analyze Rayleigh wave dispersive characteristics under point load for layered soil system. They considered the effects of body waves and higher Rayleigh modes due to irregular soil stratification, and suggested an even wider receiver spacing range: $0.5\lambda_R \le \Delta x \le 4\lambda_R$. Ganji [6] summarized and gave a list of all the criteria mentioned above. Up till now, there is still not a consistent agreement on the arrangement of source and receivers for the SASW test.

To solve the problem mentioned above, it is necessary to obtain the exact solution (displacement and stress) on surface of elastic half-space subjected to a vertical harmonic point load excitation. By comparing the exact solution with plane Rayleigh wave results for different source-to-receiver distances r, suitable r can be determined for corresponding accuracy requirement. Wang [7] gave closed form solution for this problem with Poisson's ratio of 0.25. Through comparing the amplitude of vertical displacement, Wang suggested that the Rayleigh wave approximate solution will be valid in the range of $2\pi fr/V_s \ge 3.5$, which corresponds to $r > 0.61\lambda_R$ when expressed in the form of Rayleigh wavelength. The result gives a high lower bound value than the criterion suggested by Heisey. However, this criterion was only based on amplitude analysis, and its validity should be further investigated when phase information is taken into account in the SASW test.

In this study, by investigating both amplitude and phase of surface vertical displacement, Rayleigh wave approximate solutions are compared to Wang's [7] exact solution, and the effects of source-to-receiver distance r and receiver spacing Δx on Rayleigh wave dispersion curves are discussed. For a uniform, half-space with Poisson's ratio other than 0.25, the exact solution is difficult to obtain. Therefore, in this paper, a numerical analysis is performed to calculate the dynamic response on half-space surface, and the validity condition for the plane Rayleigh wave approximation is investigated with consideration of the effect of Poisson's ratio.

2. Analytical studies

2.1. Approximate and exact solution of vertical surface displacement

To investigate dispersion of Rayleigh wave caused by point load, analytical studies of the dispersive characteristic of wave propagation in uniform half-space were conducted. For Poisson's ratio of 0.25, the far field vertical displacement solution (approximate solution) under a unit harmonic point load excitation was given by Barkan [8] as follows:

$$w(r,t) = -\frac{a_r}{Gr}e^{i\omega t}(f_{1R} + if_{2R}) \tag{2}$$

where $a_r = \omega r/V_S$, $\omega = 2\pi f$; $i = \sqrt{-1}$, G is shear modulus of soil; $f_{1R} = 0.0998Y_0(1.08777a_r)$, $f_{2R} = 0.0998J_0(1.08777a_r)$; $J_0(x)$ and $Y_0(x)$ are Bessel functions of the first and second kind of order zero, respectively.

The closed form exact solution given by Wang [7] is also rewritten in a similar form:

$$\begin{aligned} w(r,t) &= \frac{a_r e^{i\omega t}}{32\pi Gr} \\ &\quad \times\left\{\frac{6}{a_r}(e^{-i(a_r/\sqrt{3})} + e^{-ia_r}) + i(I_1 + I_2 + I_3 + I_4)\right\} \\ &= -\frac{a_r}{Gr}e^{i\omega t}(f_1 + if_2) \end{aligned} \tag{3}$$

where

$$I_1 = \sqrt{3}\int_{(1/\sqrt{3})}^{1} \frac{e^{-ia_r\tau}d\tau}{\sqrt{\tau^2 - \left(\frac{1}{2}\right)^2}},$$

$$I_2 = -\sqrt{3\sqrt{3}+5}\int_{(1/\sqrt{3})}^{1} \frac{e^{-ia_r\tau}d\tau}{\sqrt{\gamma^2 - \tau^2}},$$

$$I_3 = -\sqrt{3\sqrt{3}-5}\int_{(1/\sqrt{3})}^{1} \frac{e^{-ia_r\tau}d\tau}{\sqrt{\tau^2 - \gamma_1^2}},$$

$$I_4 = 2\sqrt{3\sqrt{3}+5}\int_{(1/\sqrt{3})}^{\gamma} \frac{e^{-ia_r\tau}d\tau}{\sqrt{\gamma^2 - \tau^2}}.$$

in which

$$\gamma = \sqrt{(3+\sqrt{3})}/2,\ \gamma_1 = \sqrt{(3-\sqrt{3})}/2.$$

2.2. Comparison of approximate solution with exact solution

Through comparing the amplitude and phase of vertical surface displacement calculated from Eqs. (2) and (3), we can estimate effect of body waves at different distances.

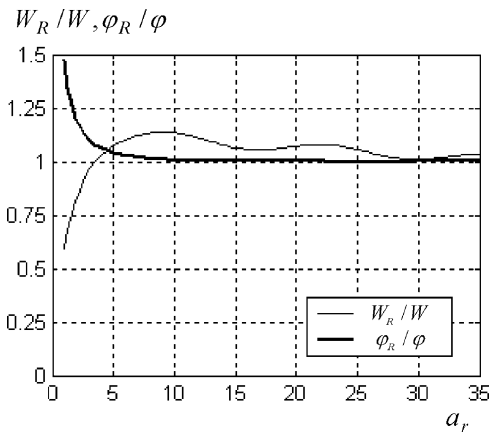

Fig. 2. W_R/W and φ_R/φ vs. a_r.

The relative amplitude and phase obtained from approximate and exact solution can be defined as: $W = \sqrt{f_1^2 + f_2^2}$, $W_R = \sqrt{f_{1R}^2 + f_{2R}^2}$; $\varphi = \tan^{-1}(f_2/f_1)$, $\varphi_R = \tan^{-1}(f_{2R}/f_{1R})$.

For the case of uniform half-space with Poisson's ratio of 0.25, W_R/W, φ_R/φ only vary with a_r. With shear wave velocity $V_S = 100$ m/s, mass density $\rho = 1700$ kg/m^3 and the excitation frequency $f = 100$ Hz, the ratios of approximate solution to exact solution are plotted vs. a_r in Fig. 2. It can be observed from Fig. 2 that the amplitude difference between approximate and exact solutions will be limited under 5% when $a_r = 2.8–4.4$ and $a_r > 25$, which is different from Wang's suggestion of $a_r > 3.5$. As to phase angle, the difference will be less than 5% when $a_r > 6$, which corresponds to $r/\lambda_R > 1$.

2.3. Effect of source and receivers on dispersion curve of Rayleigh wave

To investigate the effect of r and receiver spacing Δx on Rayleigh wave dispersion curve, phase velocities of Rayleigh wave are calculated from phase difference and spacing between two receivers using Eq. (1) and definitions of φ and φ_R. The variations are shown in Figs. 3 and 4. For

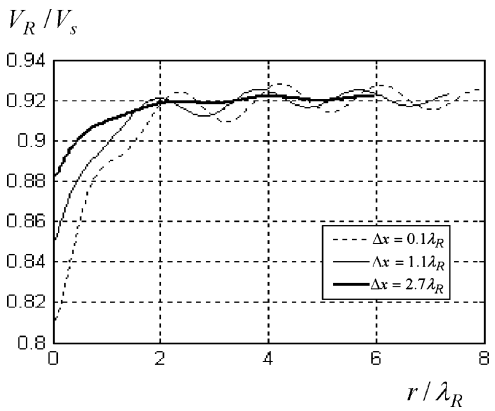

Fig. 3. Rayleigh wave dispersion curve from exact solution ($\nu = 0.25$).

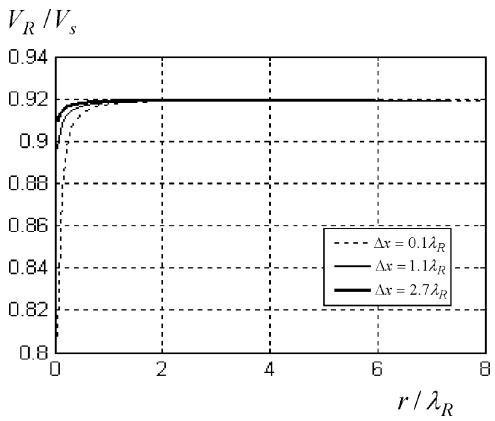

Fig. 4. Rayleigh wave dispersion curve from approximate solution ($\nu = 0.25$).

Poisson's ratio $\nu = 0.25$, the theoretical value of plane Rayleigh wave velocity is $V_R/V_S = 0.919$. The following disparities can be observed by comparing Figs. 3 and 4:

(1) For low value of r/λ_R, the calculated Rayleigh wave velocity V_R increases with increasing r, and the result of exact solution is smaller than that of approximate solution, i.e., the assumption of plane Rayleigh wave is valid only when r/λ_R reaches a certain value.
(2) There are some fluctuations in dispersion curves shown in Fig. 3, which are more pronounced for small values of $\Delta x/\lambda_R$. By comparing with Fig. 4 related to only Rayleigh wave, we believe that the fluctuations result from interference of body waves. These observations agree with results given by Sanchez-Salinero et al. [2] and Rosset et al. [3].
(3) When arrangements of source and receivers meet the requirement of $r/\lambda_R > 1$ and $\Delta x/\lambda_R \geq 0.1$, the Rayleigh wave phase velocity difference between exact solution and approximate solution is less than 4%, which decreases with the increasing $\Delta x/\lambda_R$.
(4) Smaller source-to-near-receiver distance r/λ_R can be used with increased receiver spacing $\Delta x/\lambda_R$ without increasing measurement error.

3. Numerical simulation of the SASW test

3.1. Numerical simulation model

An axisymmetric numerical model has been used to study the SASW test. The discrete mesh model is shown in Fig. 5. The finite element mesh area is r_0 by z_0, in which, 8-node isoparametric elements are used. Three kinds of infinite elements are used in analysis and are shown in Fig. 6.

The first kind of infinite element (IE1) is used to simulate wave propagation in radial uniform infinite field along horizontal direction, in which vertical displacement shape function is same as that of ordinary finite element. The radial

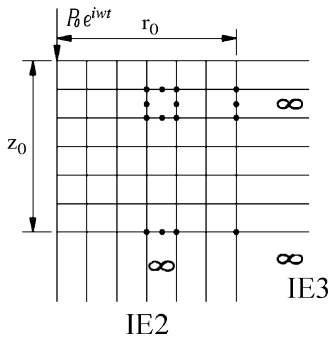

Fig. 5. Finite element mesh.

horizontal displacement is constructed based on the dynamic fundamental solution of uniform elastic half-space system, and can be expressed as

$$\{u\ w\}^T = [H][N]\{\delta\} \tag{4}$$

where

$$\{\delta\} = \{u_1 w_1 u_2 w_2 u_3 w_3\}^T,\quad [H] = \begin{bmatrix} H_1 & 0 \\ 0 & H_2 \end{bmatrix},$$

$$H_1 = H_1^{(2)}(kr)/H_1^{(2)}(kr_0),\quad H_2 = H_0^{(2)}(kr)/H_0^{(2)}(kr_0),$$

$$[N] = \begin{bmatrix} N_1 & 0 & N_2 & 0 & N_3 & 0 \\ 0 & N_1 & 0 & N_2 & 0 & N_3 \end{bmatrix},$$

$$N_1 = \eta(\eta+1)/2,\quad N_2 = 1-\eta^2,\quad N_3 = \eta(\eta-1)/2.$$

in which $H_0^{(2)}(kr)$ and $H_1^{(2)}(kr)$ are, respectively, Hankel functions of the second kind of order zero and order one, $k = \omega/V_R$ is the wave number of Rayleigh wave, while r_0 is horizontal coordinate of origin of the first kind of infinite element.

The second kind of infinite element (IE2) is used to simulate wave propagation along vertical direction, and the horizontal displacement can be defined by ordinary shape function. The vertical displacement is based on field test results and takes the form of $\exp[-\alpha(z-z_0)\lambda_P]$. Therefore, we have

$$\{u\ w\}^T = \exp[-\alpha(z-z_0)\lambda_P][N]\{\delta\} \tag{5}$$

where $\alpha = \alpha_1 + i2\pi$. According to experimental results and numerical analysis, α_1 can be taken as any value in range 1–10; the definition of $[N]$ is similar to that in Eq. (4) and defined as $N_1 = \xi(\xi-1)/2$, $N_2 = 1-\xi^2$, $N_3 = \xi(\xi-1)/2$; λ_P is wavelength of P wave, z_0 is the depth of origin of the second kind of infinite element.

The third type of infinite element (IE3) is used to simulate wave propagation in an infinite field along both horizontal and vertical directions. The displacement of element can be expressed as

$$\{u\ w\}^T = \exp[-\alpha(z-z_0)\lambda_P][H]\{\delta\} \tag{6}$$

where notations have same definitions as in Eqs. (4) and (5). The detailed stiffness and mass matrix for these kinds of infinite elements were given by Liang et al. [9].

When the vertical displacements on surface w are obtained, the phase of w for any source-to-receiver distance r can be determined from $\varphi = \arctan(w_i/w_r)$, where w_i and w_r are, respectively, the imaginary and real parts of w. When combined with Eq. (1), the Rayleigh wave velocity V_{Rt} by a point source can be calculated. The validity condition for the plane Rayleigh wave approximation can be determined by comparing dispersion curves of V_{Rt} and plane Rayleigh wave velocity V_R.

3.2. Verification of the numerical model

To verify accuracy of the numerical analysis, the results of numerical simulation are compared to Wang's exact solution for a uniform elastic half-space with Poisson's ratio of 0.25, and shown in Fig. 7. The parameters corresponding to this case (Case 1) are: $V_S = 100$ m/s (because no dispersion occurs for a uniform half-space with a given Poisson's ratio, different V_S, say 200 or 300 m/s, will lead to the same conclusion in Sections 2–4 of this paper), $\rho = 1500$ kg/m^3, finite element mesh area is $r_0 = z_0 = (1-3)\lambda_P$, element size $= \lambda_s/8$, excitation frequency $f = 100$ Hz, receiver spacing $\Delta x = 1.5\lambda_s$, where $\lambda_P = \sqrt{2(1-\nu)/(1-2\nu)}\lambda_s$ is the wavelength of P wave. According to plane Rayleigh wave theory, there will be $V_R/V_S = 0.919$. From Fig. 7, it can be seen the results of numerical analysis agree fairly well with the exact solution.

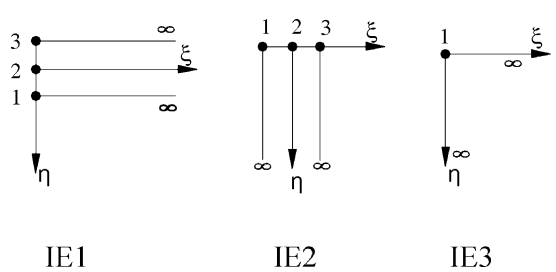

Fig. 6. Three kinds of infinite elements.

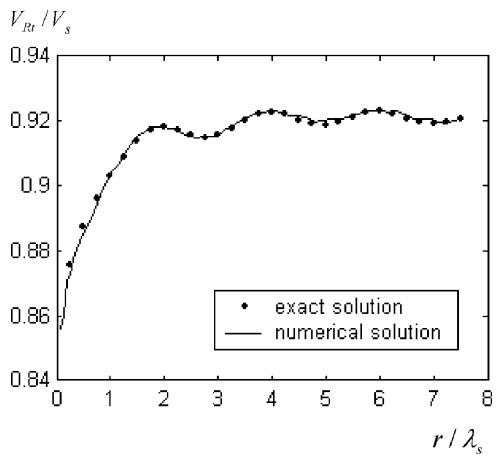

Fig. 7. Verification of numerical model ($\nu = 0.25$).

4. Parametric studies with numerical analysis

Dynamics responses and Rayleigh wave velocities of a uniform and layered half-space subjected to a unit harmonic point load excitation are analyzed with the finite–infinite element model shown in previous section. The model parameters are same as those in Case 1, except mass density $\rho = 1500$ kg/m^3 for Poisson's ratio $\nu \leq 0.25$, and $\rho = 1700$–1800 kg/m^3 for $\nu \geq 0.35$. The effect of source-to-near-receiver distance r, receiver spacing Δx and Poisson's ratio ν are investigated, and the results are shown in Fig. 8.

4.1. Effect of Poisson's ratio

For $\nu \leq 0.25$, Fig. 8a and b show some common patterns. Rayleigh wave velocity increases with increasing r/λ_R in

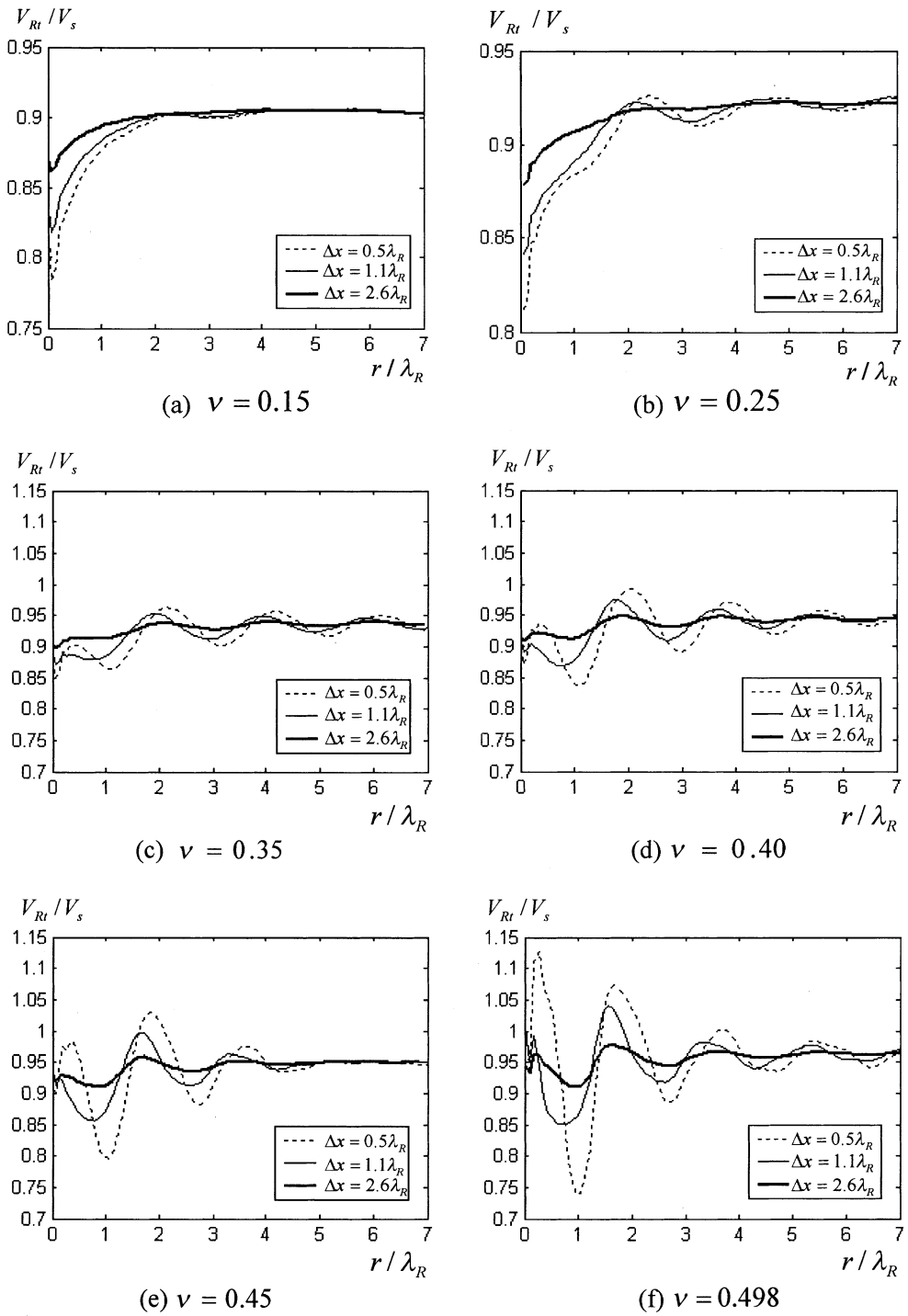

Fig. 8. Variation of Rayleigh wave phase velocity with r/λ_R, $\Delta x/\lambda_R$ and Poisson's ratios.

the range of small value of r/λ_R, which agrees with previous analytical analysis. However, for large Poisson's ratio $\nu \geq 0.35$, there are significant fluctuations in dispersion curves, and the oscillations are more pronounced with increasing ν and decreasing $\Delta x/\lambda_R$. The dispersion curves are shown in Fig. 8c–f for $\nu = 0.35$, 0.40, 0.45 and 0.498. According to Eq. (1), using larger Δx is equivalent to a linear average of $\varphi - r$ curve between two receivers, therefore, the oscillation can be reduced by increasing Δx.

From the discussion of previous section, the fluctuations in dispersion curve result from interference of body waves. For soils with a high Poisson's ratio or saturated soils, Poisson's ratio will be in the range 0.49–0.5. According to elastic wave theory, in this situation, the corresponding wavelength of P waves will be much larger than that for $\nu = 0.25$, and reaches $\lambda_P > 7.5\lambda_R$. Therefore, the geometrical attenuation of energy related to P waves will be rather lower for large ν. As discussed before, for $\nu \leq 0.25$, the assumption of plane Rayleigh wave is valid for $r/\lambda_R > 1$; however, for large Poisson's ratio, say $\nu \geq 0.35$, larger value of r/λ_R is needed for the validity of plane Rayleigh wave assumption. From these analyses, we can also conclude that P waves are the major contributions to the oscillations in Rayleigh wave dispersion curves.

4.2. Source-to-receiver distance and receiver spacing

A major goal of SASW test is to estimate shear moduli of soil from estimated shear wave velocities by using $G = \rho V_S^2$. Obviously, the errors in estimating shear modulus will double the errors in measuring V_S. If we set the maximum acceptable error in estimating shear modulus as 10%, then the error in calculation for the Rayleigh wave velocity must be controlled within 5%. The receiver arrangements satisfying these error requirements are listed in Table 1. It can be seen that when there is a receiver spacing setup $\Delta x/\lambda_R = 0.5$ for $\nu \leq 0.25$ and $\nu \geq 0.35$, the allowable minimum values of r/λ_R are 0.67 and 1.42–2.95, respectively. When $\Delta x/\lambda_R = 2.6$, for any value of Poisson's ratio, there is no limitation to r/λ_R, i.e., choosing any value of r/λ_R can keep the error of V_R within 5%. Therefore, for a specific error requirement, the minimum values of r/λ_R can be decreased with increasing $\Delta x/\lambda_R$ and decreasing of ν. For more strict error control requirement, larger values of r/λ_R should be used than the values given in Table 1.

Table 1
Allowable minimum value of r/λ_R when V_R measurement error $\leq 5\%$

ν	0.15–0.25	0.35–0.40	0.40–0.498
$\Delta x/\lambda_R$			
0.5	0.67	1.42	2.95
1.1	0.42	1.11	1.81
2.6	The values being chosen at random		

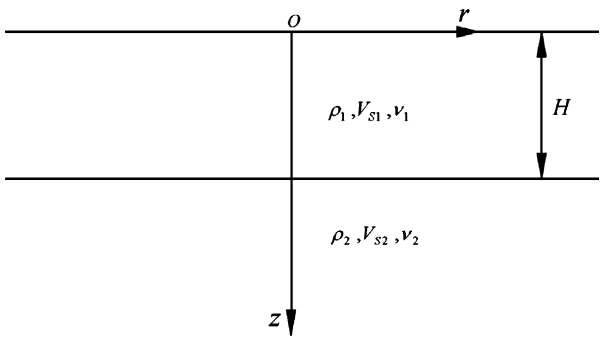

Fig. 9. Two-layered stratum.

4.3. Effect of soil stratification

To study the effect of soil stratification, the model shown in Fig. 9 was analyzed. A surface layer with thickness $H = 3$ m and shear wave velocity $V_{s1} = 100$ m/s is underlain by a half-space with $V_{s2} = 200$ m/s. The influence of saturation degree of the underlying soil is considered by using different Poisson's ratios. Unsaturated soil strata are represented with $\nu_1 = \nu_2 = 0.35$, $\rho_1 = \rho_2 = 1400$ kg/m^3; while for the underlying soil saturated, $\nu_2 = 0.498$ and $\rho_2 = 1700$ kg/m^3. From the plane Rayleigh waves theory, we know that the Rayleigh wave velocity V_{Rt} will approach the Rayleigh wave velocity of surface layer V_{R1} when frequency $f \rightarrow \infty$ and the velocity of the underlying half-space V_{R2} when $f \rightarrow 0$, respectively.

With the corresponding plane Rayleigh wave velocity V_R in parentheses, Figs. 10 and 11 show the influences of r/λ_R, $\Delta x/\lambda_R$ and Poisson's ratio ν_2 on Rayleigh wave velocity V_{Rt} at frequencies $f = 5$ and $f = 25$ Hz (wavelengths are, respectively, about 35.5 and 3.8 m). It can be seen that the results agree with the plane Rayleigh wave theory at large r/λ_R and $\Delta x/\lambda_R$. It is also noted that the soil stratification leads to significant fluctuations in these curves, and the oscillation amplitudes attenuate with increased value of r/λ_R. Further investigating Figs. 10a and 11a, we can find the attenuation rate becomes slower when the Poisson's ratio of soil increases. Therefore, when the SASW test is performed on layered soil systems, larger source-to-near receiver distances r/λ_R than those used in uniform soil tests should be adopted to obtain reliable results. In addition, much lower oscillation amplitudes are observed for $\Delta x/\lambda_R = 2.5$ than for $\Delta x/\lambda_R = 0.5$ in Figs. 10 and 11, which indicates that using larger receiver spacing $\Delta x/\lambda_R$ also helps reducing the effect of r/λ_R on Rayleigh wave velocity measurement.

5. Conclusions

This paper provides an analytical analysis and numerical simulation of the SASW test method to investigate errors in calculating Rayleigh wave velocity due to plane Rayleigh

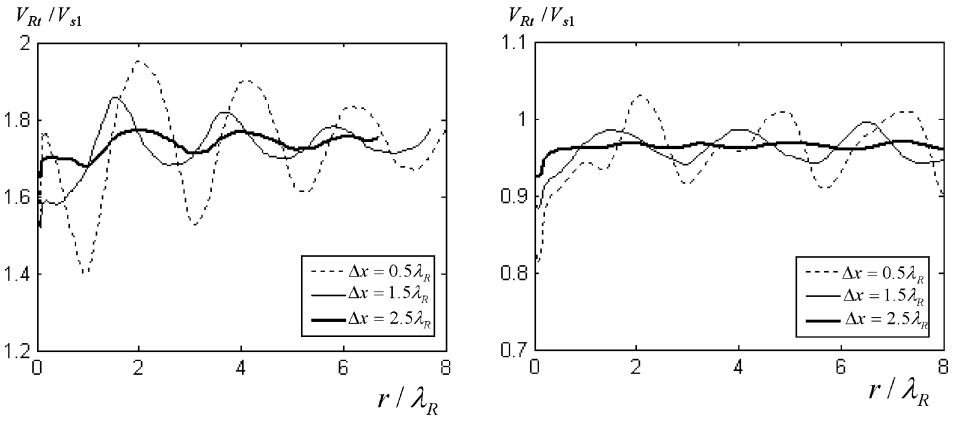

Fig. 10. R-wave velocity curves vs. r/λ_R with $\nu_2 = 0.35$ for layered stratum.

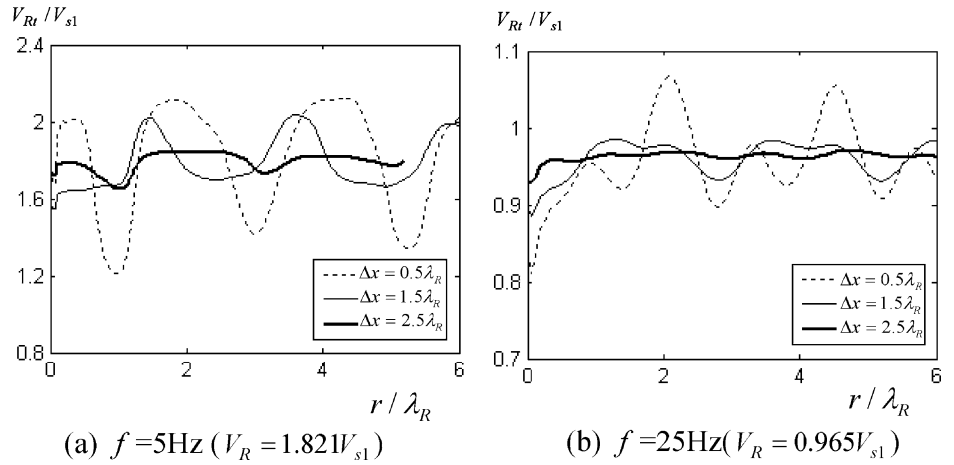

Fig. 11. R-wave velocity curves vs. r/λ_R with $\nu_2 = 0.498$ for layered stratum.

wave assumption. The following conclusions are drawn from the study:

(1) Plane Rayleigh wave assumption is valid only when the source and receiver arrangement r/λ_R, $\Delta x/\lambda_R$ meet certain criteria, which are significantly affected by Poisson's ratio or saturation degree of soil.
(2) For large Poisson's ratios or small $\Delta x/\lambda_R$, Heisey's filtering criterion may cause very large error in V_R measurement.
(3) In the SASW testing, it is unnecessary to keep $r = \Delta x$. For the case of $\nu \leq 0.25$ and $r/\lambda_R > 1$, any value of $\Delta x/\lambda_R$ can keep the error in V_R measurement within 4%.
(4) When receiver spacing is large enough, for example, $\Delta x/\lambda_R = 2.6$, for any value of Poisson's ratio ν and source-to-near-receiver distance r, the errors in V_R measurement can be controlled within 5%.
(5) For stratified soil system, using large r/λ_R and $\Delta x/\lambda_R$ also helps improving measurement reliability and precision.

Although using large receiver spacing can simplify the source-to-near-receiver distance configuration, the risk of making a mistake in phase correction (phase unwrapping) rises because the phase of the cross-power spectrum ranges $-\pi - +\pi$, especially when the soil profile is unclear. It may also increase the requirement for source power and reduce signal quality. A multi-channel signal detection method with smaller receiver spacing ($\Delta x/\lambda_R < 1$) can be used to solve these problems, where signals collected from every two adjacent receivers are averaged. Therefore, the results of this study also provide a theoretical proof to the advantage of multichannel analysis of surface waves (MASW).

Acknowledgements

This research is supported by the National Natural Science Foundation of China (Grant No. 50079027).

References

[1] Heisey, J.S., Stokoe, K.H., II, Hudson, W.R., Meyer, A.H., 1982. Determination of in situ shear wave velocities from Spectral Analysis of Surface Waves, Research Report 256-2, Center for Transportation Research, Univ. of Texas at Austin, 277 pp.

[2] Sanchez-Salinero I, Rosset JM, Shao KY, Stokoe II KH, Rix GJ. Analytical evaluation of variables affecting surface wave testing of pavements. Transport Res Rec 1987;1136:86–95.
[3] Rosset JM, Chang DW, Stokoe II KH, Aouad M. Modulus and thickness of the pavement surface layer from SASW tests. Transport Res Rec 1989;1260:53–63.
[4] Hiltunen DR, Woods RD. Variables affecting the testing of pavements by the surface wave method. Transport Res Rec 1989; 1260:42–52.
[5] Gucunski N, Woods RD. Numerical simulation of the SASW test. Soil Dyn Earthquake Engng 1992;11(4):213–27.
[6] Ganji V, Gucunski N, Nazarian S. Automated inversion procedure for spectral analysis of surface waves. J Geotech Engng, ASCE 1998; 124(8):757–70.
[7] Wang YS. Exact solution for the dynamic vertical surface displacement of the elastic half-space under vertical harmonic point load. Acta Mech Sin 1980;12(4):386–91. in Chinese.
[8] Barkan DD. Dynamics of Bases and Foundation. New York: McGraw-Hill; 1962. p. 331–8.
[9] Liang GQ, Chen LZ, Wu SM. Boundary processing of semi-infinite space for solving axisymmetrical dynamic problems. Chin J Geotech Engng 1995;17(3):19–25. in Chinese.